RUNX3 Attenuates β-Catenin/T Cell Factors in Intestinal Tumorigenesis

Kosei Ito,[1,2,4] Anthony Chee-Beng Lim,[1] Manuel Salto-Tellez,[2] Lena Motoda,[1] Motomi Osato,[1,2] Linda Shyue
Huey Chuang,[1] Cecilia Wei Lin Lee,[1] Dominic Chih-Cheng Voon,[1] Jason Kin Wai Koo,[2] Huajing Wang,[2]
Hiroshi Fukamachi,[3] and Yoshiaki Ito[1,2,*]
[1]Institute of Molecular and Cell Biology, Proteos, 61 Biopolis Drive, Singapore 138673
[2]Oncology Research Institute, Yong Loo Lin School of Medicine, National University of Singapore, 28 Medical Drive, Singapore 117456
[3]Department of Molecular Oncology, Tokyo Medical and Dental University, Yushima 1-5-45, Bunkyo-ku, Tokyo 113-8519, Japan
[4]Present address: Graduate School of Biomedical Sciences, Nagasaki University, 1-7-1 Sakamoto, Nagasaki 852-8588, Japan
*Correspondence: itoy@imcb.a-star.edu.sg
DOI 10.1016/j.ccr.2008.08.004

SUMMARY

In intestinal epithelial cells, inactivation of APC, a key regulator of the Wnt pathway, activates β-catenin to initiate tumorigenesis. However, other alterations may be involved in intestinal tumorigenesis. Here we found that RUNX3, a gastric tumor suppressor, forms a ternary complex with β-catenin/TCF4 and attenuates Wnt signaling activity. A significant fraction of human sporadic colorectal adenomas and $Runx3^{+/-}$ mouse intestinal adenomas showed inactivation of RUNX3 without apparent β-catenin accumulation, indicating that RUNX3 inactivation independently induces intestinal adenomas. In human colon cancers, RUNX3 is frequently inactivated with concomitant β-catenin accumulation, suggesting that adenomas induced by inactivation of RUNX3 may progress to malignancy. Taken together, these data demonstrate that RUNX3 functions as a tumor suppressor by attenuating Wnt signaling.

INTRODUCTION

Multiple genetic changes have been observed in colon carcinogenesis. In familial adenomatous polyposis coli (FAP), affected individuals carry heterozygous mutations of the APC gene, which encodes a key regulator of the canonical Wnt pathway that destabilizes β-catenin, one of the Wnt pathway's nuclear effectors. Adenomas caused by biallelic inactivation of APC show nuclear and cytoplasmic accumulation of β-catenin. In colorectal cancers with stabilized β-catenin, the β-catenin/T cell factor 4 (TCF4) transcription factor complex is constitutively activated. It has been widely surmised that oncogenic Wnt signaling initiates colorectal carcinogenesis (Kinzler and Vogelstein, 1996). However, studies of sporadic cases of colorectal cancer and analyses of aberrant crypt foci (ACF)—the proposed precursors of adenomas—have suggested that alterations other than inactivation of APC or activation of β-catenin may be involved (Jass et al., 2002). These alterations could implicate alternative mechanisms for the activation of Wnt signaling.

The TGF-β pathway is another key pathway that influences the growth and differentiation of gut epithelial cells and is altered in gastrointestinal cancers (Mishra et al., 2005). Several components of the TGF-β signaling cascade are bona fide tumor suppressors that inhibit cell growth and cancer development. Inactivation of one of these components, such as the TGF-β receptor type II or Smad4, occurs frequently in gastrointestinal tumors (Derynck et al., 2001). However, the molecular mechanisms that link the oncogenic Wnt and the tumor-suppressive TGF-β pathways in intestinal carcinogenesis have not been fully elucidated.

RUNX3 is inactivated by gene silencing or protein mislocalization in more than 80% of gastric cancers (Li et al., 2002; Ito et al., 2005). More recently, inactivation of RUNX3 was reported in a wide range of other cancer types (Blyth et al., 2005). The RUNX3 locus at 1p36, a region that undergoes frequent allelic loss in gastrointestinal cancers, is silenced by promoter hypermethylation in a significant proportion of cancer-derived cell lines and clinical specimens, suggesting that it fulfills

SIGNIFICANCE

It is known that biallelic inactivation of APC induces colon adenomas. We found that biallelic inactivation of RUNX3 without nuclear/cytoplasmic accumulation of β-catenin also induces colon adenomas. Our results suggest that APC and RUNX3 may function independently as gatekeepers in colon adenoma development. Wnt signaling is an oncogenic pathway, whereas TGF-β signaling is a tumor suppressor pathway. The nuclear effectors of these pathways, β-catenin/TCF4 and RUNX3, respectively, form a ternary complex with decreased DNA-binding ability. This ternary complex appears to integrate growth-promoting and cytostatic signals for homeostatic balance of growth and differentiation in intestinal epithelial cells.

a tumor-suppressive function in colorectal cancers (Goel et al., 2004; Ku et al., 2004). RUNX3 regulates target gene expression by forming a complex with Smad molecules. We reported previously that *Runx3*^{−/−} gastric epithelial cells are resistant to the growth-inhibitory and apoptosis-inducing properties of TGF-β, suggesting that RUNX3 is a downstream effector of the TGF-β family signaling pathway. Furthermore, TGF-β regulates nuclear translocation of RUNX3 in gastric epithelial cells (Ito et al., 2005) and activates the transcription of *p21*[WAF1/Cip1] and *Bim*, a negative cell-cycle regulator and a proapoptotic gene, respectively, in cooperation with RUNX3 and Smads (Chi et al., 2005; Yano et al., 2006; reviewed in Ito, 2008).

In this study, we investigated possible roles of RUNX3 in regulating the Wnt pathway and in intestinal tumorigenesis.

RESULTS

β-Catenin/Tcf4 Activity Is Increased in *Runx3*^{−/−} Mouse Intestine

Runx3 protein was detected in the epithelial cells of mouse small and large intestines (Figures 1A and 1B). Runx3 is expressed in all epithelial cell types in the small intestine, except in Paneth cells, whose maturation is induced by Wnt signaling and accompanied by nuclear accumulation of β-catenin (Figure 1A; van Es et al., 2005; Andreu et al., 2005). We reported previously that *Runx3*^{−/−} mice on the C57BL/6 background die soon after birth due to starvation (Li et al., 2002). However, some *Runx3*^{−/−} mice on the BALB/c background survive for about 10–12 months. We analyzed these survivors at the adult stage.

Adult and neonate *Runx3*^{−/−} epithelia of the small and large intestines show high proliferation (Figures 1D and 1E), and epithelia of adult *Runx3*^{−/−} mice show hyperplasia (Figure 1C; see also Figure S1A available online). Cell lines obtained from *Runx3*^{−/−} small and large intestinal epithelium (FID and FIL cell lines, respectively) grew faster on monolayer cultures than those from *Runx3*^{+/+} mice (Figure 1F for FID; data not shown for FIL). No tumors formed in the intestines of *Runx3*^{−/−} mice, which die at around 10–12 months of age. However, small intestinal adenomas developed in *Runx3*^{+/−} mice at about 65 weeks of age. (Analyses of *Runx3*^{+/−} intestine are described below.)

The proliferation of intestinal epithelial cells is known to be accelerated by Wnt/β-catenin/Tcf4 signaling. Therefore, we examined whether Wnt signaling is activated in *Runx3*^{−/−} intestinal epithelial cells. Target genes known to be positively regulated by β-catenin/Tcf4, such as CD44, cyclin D1, c-Myc, conductin, and EphB2 (He et al., 1998; Tetsu and McCormick, 1999; Batlle et al., 2002; van de Wetering et al., 2002), were upregulated in the ileum, jejunum, and colon (Figures 1G and 1I; Figure S1B), while a gene negatively regulated by β-catenin/Tcf4, EphrinB1 (Batlle et al., 2002), was downregulated in epithelial cells of *Runx3*^{−/−} intestine (Figures 1G and 1I).

It has been demonstrated that the EphB/EphrinB system controls the positioning of epithelial cells within the small intestinal mucosa (Batlle et al., 2002). Enhanced β-catenin/Tcf4 activity in *Apc*-deficient small intestine where the EphB/EphrinB system is dysregulated causes displacement of epithelial cells (Sansom et al., 2004; Andreu et al., 2005). This is clearly shown by the random localization of Paneth cells, which are normally tightly clustered at the bottom of the gland (Batlle et al., 2002). We observed

that Paneth cells were distributed throughout the villi in *Runx3*^{−/−} small intestine (Figure 1H). It is noteworthy that the levels of β-catenin and Tcf4 were not noticeably altered in intestinal epithelial cells of *Runx3*^{−/−} mice compared to those of wild-type (WT) mice (Figure 1I), indicating that the increase in Wnt signaling activity in *Runx3*^{−/−} intestinal epithelial cells is not due to an increase in the levels of these proteins. Furthermore, *Runx3*^{−/−} FID cells showed higher sensitivity to Wnt3a stimulation than *Runx3*^{+/+} cells (Figure 1J). This increased β-catenin/Tcf4 activity of *Runx3*^{−/−} cells after Wnt3a treatment was supported by electrophoresis mobility shift assays (EMSAs), which showed increased β-catenin/Tcf4 complexes bound to the TCF site after Wnt3a treatment (Figure S3B).

Taken together, these results suggest that Runx3 regulates Wnt signaling activity negatively.

RUNX3 Forms a Ternary Complex with β-Catenin and TCF4

Since β-catenin and Tcf4 levels were unaffected in *Runx3*^{−/−} intestinal epithelial cells (Figure 1I), we investigated whether RUNX3 directly inhibits the function of β-catenin/TCF4. We examined 22 well-characterized human colon cancer cell lines for expression of RUNX3 (Figure 2A). Only 8 cell lines, HCT116, SW480, COLO320, SW403, SW837, CCK81, SW620, and RCM1, expressed RUNX3. We found that exogenously expressed TCF4, β-catenin, and RUNX3 coimmunoprecipitated in HCT116 (Figure 2B) and 293T cells (data not shown) and that they formed a ternary complex as revealed by a two-step coimmunoprecipitation (Figure 2C). The endogenous ternary complex was also detected in DNA-free nuclear extracts of HCT116 and SW620 cells, which express dephosphorylated (activated) β-catenin and TCF4 as well as RUNX3 in the nucleus (Figure 2D). RUNX3 coimmunoprecipitated with TCF4 migrated slower than RUNX3 immunoprecipitated with anti-RUNX3 or anti-β-catenin, the reason for which is unknown. Of note, RUNX3 and TCF4 did not interact in SW480 cells (see below). Interactions between RUNX3 and TCF4 and between RUNX3 and β-catenin were also observed in a cell-free system (Figure 2E). Since β-catenin and TCF4 directly interact, our results suggest that each component in the ternary complex interacts directly with the other two. Mapping experiments revealed that the DNA-binding domains of RUNX3, the Runt domain, and TCF4, the HMG box, are required for the interaction between RUNX3 and TCF4 (Figures S2A and S2B). This result is similar to an earlier report that the interaction between Runx2 and Lef1 occurs through their respective DNA-binding domains (Kahler and Westendorf, 2003). RUNX3 was also found to interact with TCF1, TCF3, and Lef1 (Figure S2C). Interestingly, comparatively larger amounts of the active β-catenin mutants Δ45 and S33Y (Morin et al., 1997) interacted with RUNX3 than did wild-type β-catenin (Figure 2F).

RUNX3 Attenuates the Transactivational Potential of β-Catenin/TCF4

To elucidate the consequences of the interaction of RUNX3 with β-catenin/TCF4, we examined the transactivation activity of β-catenin/TCF4. In DLD1 cells, increasing the amount of exogenous RUNX3 progressively repressed the expression of a TOPflash reporter (Figure 2G). Similarly, increasing the amount of exogenous RUNX3 progressively repressed activity of the
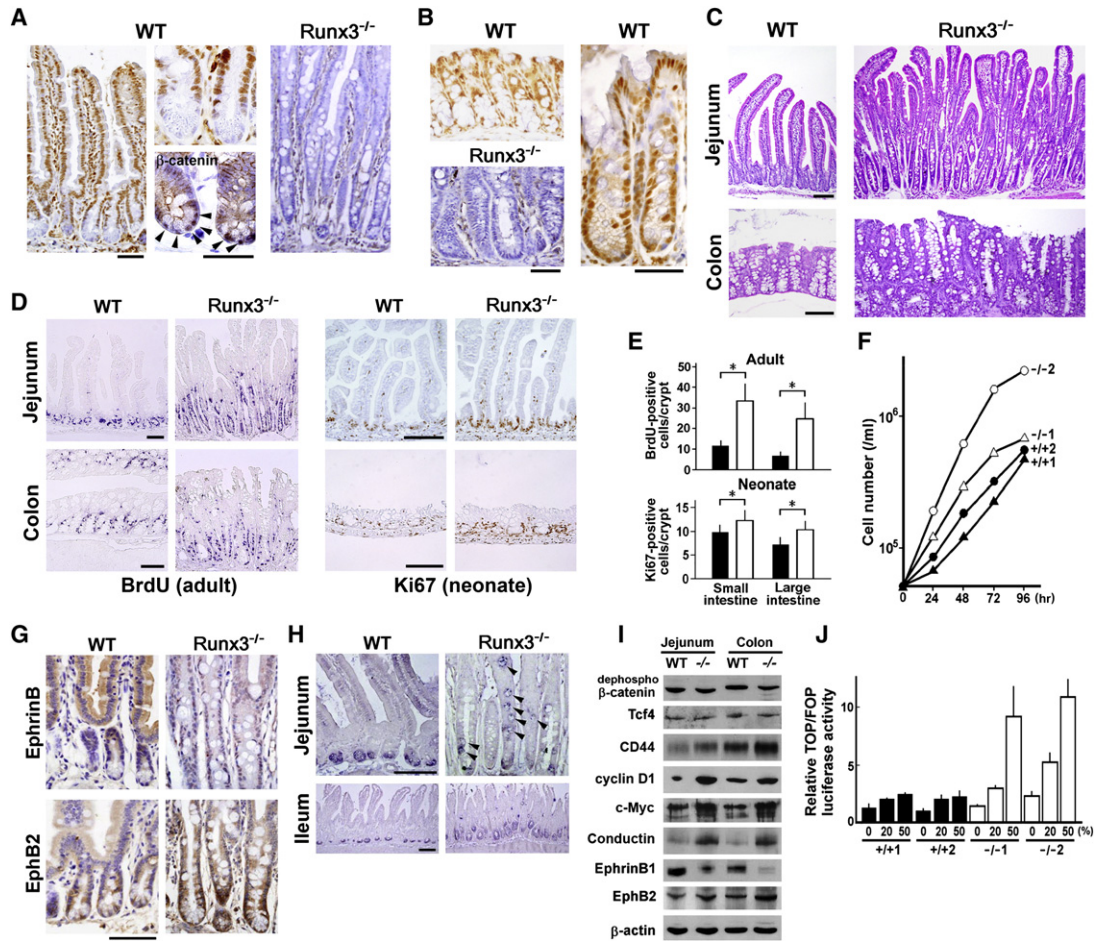
Figure 1. Expression of Runx3 in Intestinal Epithelial Cells and Upregulation of β-Catenin/Tcf4 Activity in *Runx3*$^{-/-}$ Intestine

(A) Immunodetection of Runx3 in wild-type (WT) and *Runx3*$^{-/-}$ jejunum. Note that Runx3 expression is greatly reduced in Paneth cells (upper middle panel). β-catenin is detected in the nuclei of these cells (arrowheads).

(B) Immunodetection of Runx3 in WT and *Runx3*$^{-/-}$ proximal colon (left) and WT distal colon (right).

(C) Hematoxylin and eosin (H&E) staining of WT and *Runx3*$^{-/-}$ jejunum and proximal colon of mice at 40 weeks of age.

(D) Detection of proliferating cells in WT and *Runx3*$^{-/-}$ jejunum and proximal colon by BrdU incorporation (adult; 40 weeks old) and immunostaining with anti-Ki67 antibody (neonate).

(E) Number of BrdU-positive (adult) and Ki67-positive (neonate) cells per crypt in WT and *Runx3*$^{-/-}$ intestine. *p < 0.001.

(F) Relative growth rates of *Runx3*$^{+/+}$ (+/+1 and +/+2) and *Runx3*$^{-/-}$ (−/−1 and −/−2) FID cell lines in monolayer culture.

(G) Immunodetection of EphrinB and EphB2 in WT and *Runx3*$^{-/-}$ jejunal epithelium.

(H) Immunodetection of Paneth cells with anti-lysozyme antibody in WT and *Runx3*$^{-/-}$ small intestine. Arrowheads show mispositioning of Paneth cells in *Runx3*$^{-/-}$ small intestine.

(I) Western blot analysis of protein expression profiles in WT and *Runx3*$^{-/-}$ intestine.

(J) Differential sensitivities of *Runx3*$^{+/+}$ (+/+1 and +/+2) and *Runx3*$^{-/-}$ (−/−1 and −/−2) FID cell lines to Wnt3a as evaluated by their relative TOP/FOP luciferase activities (in arbitrary units). Cells were stimulated with medium containing 20% or 50% Wnt3a-conditioned medium.

Specimens were counterstained with hematoxylin in (A), (B), and (G). Error bars represent SEM in (E) and (J). Scale bars = 50 μm in (A), (B), and (G) and 100 μm in (C), (D), (H).

wild-type *cyclin D1* promoter to a level comparable to that of the promoter lacking the TCF binding site (Figure 2H; Lin et al., 2000). The *cyclin D1* reporter construct lacks RUNX binding sites within the promoter region.

We next investigated whether the DNA-binding activity was required for RUNX3 to function as an attenuator of β-catenin/TCF4. The RUNX mutant RUNX3(R178Q) lacks DNA-binding activity and hence transactivation activity (Inoue et al., 2007). This mutant interacted with β-catenin and TCF4 (Figure 2I) and attenuated β-catenin/TCF transactivation like wild-type RUNX3

(Figure 2J), suggesting that RUNX3 directly inhibits the activity of β-catenin/TCF4 independently of its DNA-binding activity.

RUNX3 Attenuates the DNA-Binding Activity of β-Catenin/TCF4

β-catenin/TCF4 bound efficiently to consensus TCF binding sites in the *cyclin D1* and c-*Myc* promoters (Figure 3A, lanes 4 and 7) in DLD1 cells, as reported previously (Nateri et al., 2005). However, when RUNX3 was stably expressed in DLD1 cells, β-catenin/TCF4 binding to either promoter was greatly
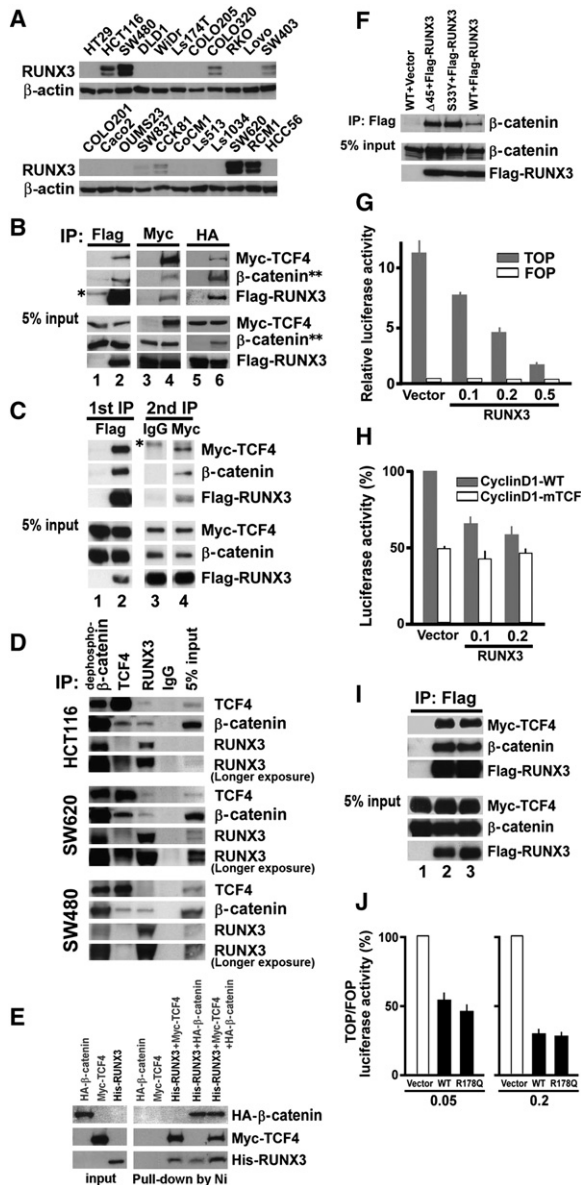
Figure 2. Detection of a β-Catenin/TCF4/RUNX3 Ternary Complex and the Attenuation of β-Catenin/TCF4 Transcriptional Activity by RUNX3

(A) Western blot analysis of RUNX3 expression in 22 human colorectal cancer cell lines.

(B) Exogenously expressed β-catenin, TCF4, and RUNX3 coimmunoprecipitate. HCT116 cells were transfected with Myc-TCF4 and vector (lane 1), Myc-TCF4 and FLAG-RUNX3 (lane 2), FLAG-RUNX3 and vector (lane 3), FLAG-RUNX3 and Myc-TCF4 (lane 4), Myc-TCF4, FLAG-RUNX3, and vector (lane 5), or Myc-TCF4, FLAG-RUNX3, and HA-β-catenin (lane 6). Proteins were immunoprecipitated with anti-FLAG agarose (lanes 1 and 2), anti-Myc (lanes 3 and 4), or anti-HA (lanes 5 and 6) antibodies, and the immunoprecipitates were subjected to western blot analysis using anti-Myc, anti-β-catenin, anti-HA, and anti-FLAG antibodies. * indicates detection of murine IgG (lanes 1 and 2). ** indicates that anti-β-catenin (for endogenous β-catenin; lanes 1–4) and anti-HA (for exogenous HA-β-catenin; lanes 5 and 6) antibodies were used.

(C) Ternary complex of exogenously expressed β-catenin/TCF4/RUNX3 detected by two-step coimmunoprecipitation. 293T cells were transfected with Myc-TCF4, S33Y β-catenin, and control vector (lane 1) or Myc-TCF4, S33Y

reduced (Figure 3A, lanes 3 and 6, and Figure 3D), and c-Myc and cyclin D1 protein levels (Figure 3E) and the expression of a TOPflash reporter were consequently lower (Figure 3G). In contrast, when RUNX3 expression was inhibited by antisense *RUNX3* in HCT116 cells, the binding of β-catenin/TCF4 to these promoters was enhanced (Figures 3B and 3D) with concomitant upregulation of c-Myc and cyclin D1 (Figure 3E) and TOPflash reporter expression (Figure 3G). Since the levels of TCF4 and dephosphorylated β-catenin were unaffected in both cases (Figure 3E), the inhibition of β-catenin/TCF4 binding to these promoters depended mainly on the level of RUNX3 expression (Figure 3C). Consistent with these observations, exogenous expression of RUNX3 downregulated the target genes of canonical Wnt signaling *AXIN2*, *CD44*, and *DKK1* in DLD1 cells, while knockdown of RUNX3 in HCT116 cells had the opposite effect (Figure 3F). Using three independent shRNAs to knockdown RUNX3, we observed a consistent inhibitory effect of RUNX3 on the expression of a TOPflash reporter in HCT116, SW620, and COLO320 cells, but not in SW480 or SW403 cells (Figure 3H). Interestingly, RUNX3 in SW480 cells did not interact with TCF4 (Figure 2D), whereas RUNX3 in SW403 cells was mislocalized to the cytoplasm (see below). These results further strengthen our conclusion that RUNX3 attenuates Wnt activity by interacting with β-catenin/TCF4 (see Discussion).

Additionally, EMSA using a DNA probe containing a consensus TCF site showed that RUNX3 inhibited the binding of TCF4 and

---

β-catenin, and FLAG-RUNX3 (lane 2). Proteins were immunoprecipitated with anti-FLAG agarose (1st IP). Bound proteins were eluted with FLAG peptide and immunoprecipitated with normal mouse IgG (lane 3) or anti-Myc antibody (lane 4) (2nd IP). 1st IP and 2nd IP were subjected to western blot analysis using anti-Myc, anti-β-catenin, and anti-FLAG antibodies. * indicates nonspecific band (lanes 3 and 4).

(D) Endogenous ternary complex of β-catenin/TCF4/RUNX3 in HCT116 and SW620 cells, but not in SW480 cells. Nuclear extracts were immunoprecipitated with anti-dephospho-β-catenin (activated β-catenin) antibody, anti-TCF4 antibody, anti-RUNX3 antibody, and normal murine IgG. The immunoprecipitates were subjected to western blot analysis using anti-dephospho-β-catenin, anti-TCF4, and anti-RUNX3 antibodies.

(E) Interaction of in vitro-translated His-tagged RUNX3 with in vitro-translated Myc-TCF4 and/or HA-β-catenin as revealed by pull-down assays with Ni-NTA agarose. Western blot analysis was performed using anti-HA, anti-His, and anti-Myc antibodies.

(F) Oncogenic β-catenins have a higher affinity for RUNX3 than wild-type β-catenin. HCT116 cells were transfected with wild-type β-catenin, Δ45 β-catenin, or S33Y β-catenin, together with FLAG-RUNX3 or control vector. Proteins immunoprecipitated with anti-FLAG agarose were subjected to western blot analysis using anti-β-catenin antibody.

(G) Reduction of TOPflash (0.1 μg DNA) activity by exogenous RUNX3 (0.1, 0.2, and 0.5 μg DNA) in DLD1 cells.

(H) Exogenous RUNX3 (0.1 and 0.2 μg DNA) reduces the activity of the wild-type *cyclin D1* promoter (CyclinD1-WT; 0.1 μg), but not that of a variant promoter with a mutated TCF binding site (CyclinD1-mTCF; 0.1 μg).

(I) Interaction of RUNX3(R178Q) with β-catenin/TCF4. 293T cells were transfected with Myc-TCF4 and S33Y β-catenin together with control vector (lane 1), FLAG-RUNX3 (lane 2), or FLAG-RUNX3(R178Q) (lane 3). Proteins were immunoprecipitated with anti-FLAG agarose. Immunoprecipitates were subjected to western blot analysis using anti-Myc, anti-β-catenin, and anti-FLAG antibodies.

(J) Reduction of TOPflash (0.1 μg DNA) activity by exogenous wild-type (WT) RUNX3 and RUNX3(R178Q) (0.05 and 0.2 μg DNA) in DLD1 cells. Error bars represent SEM in (G), (H), and (J).
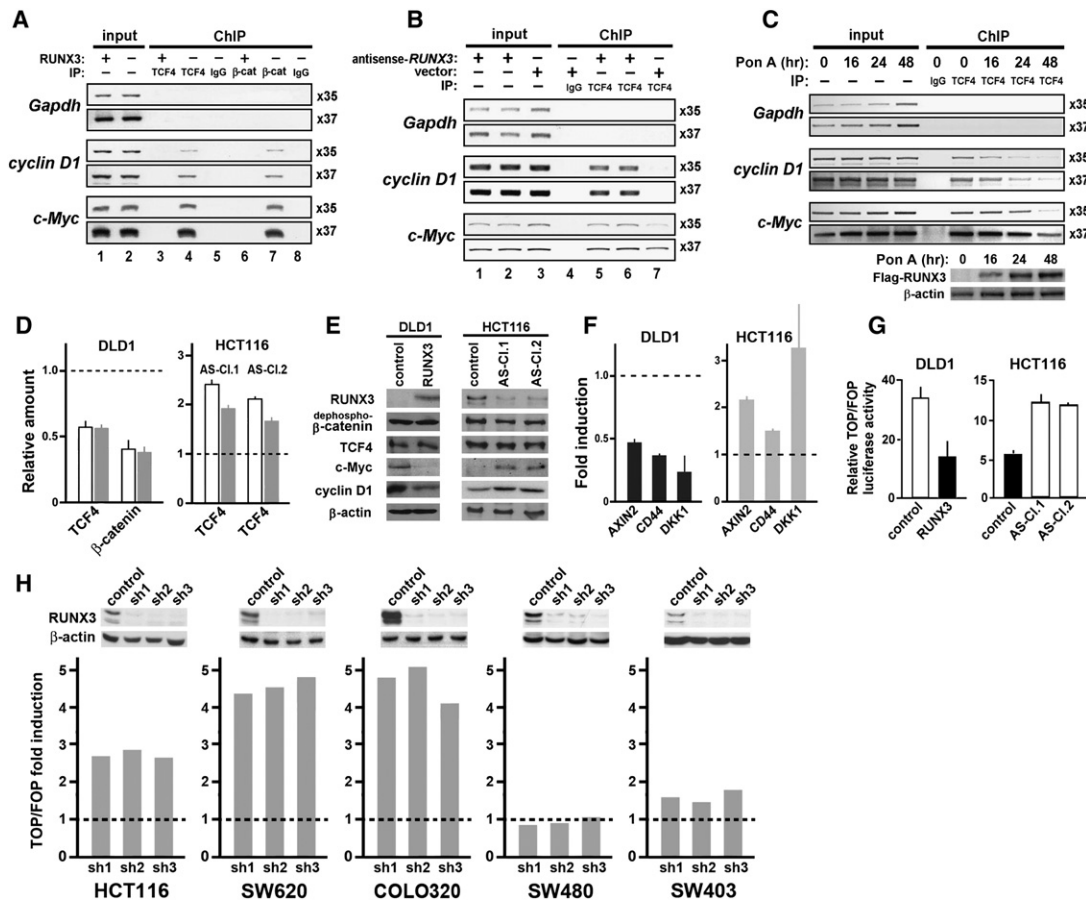
Figure 3. RUNX3 Attenuates the DNA-Binding Activity of β-Catenin/TCF4

(A) Exogenous RUNX3 attenuates the binding of β-catenin/TCF4 to TCF binding sites of the *cyclin D1* and c-*Myc* promoters. DLD1 clones expressing exogenous RUNX3 (+) or control vector (−) (see [E]) were subjected to ChIP analysis using antibodies against TCF4 (lanes 3 and 4), dephospho-β-catenin (lanes 6 and 7), or normal murine IgG (lanes 5 and 8). DNA precipitates were amplified by PCR (35 or 37 cycles).

(B) Enhanced occupancy of β-catenin/TCF4 at TCF binding sites of the *cyclin D1* and c-*Myc* promoters following RUNX3 knockdown. HCT116 clones expressing antisense DNA against *RUNX3* (AS-Cl.1, lanes 1 and 5, and AS-Cl.2, lanes 2 and 6) or control vector (control; lanes 3, 4, and 7) (see [E]) were subjected to ChIP analysis using anti-TCF4 antibodies (lanes 5–7) or normal murine IgG (lane 4). DNA precipitates were amplified by PCR (35 or 37 cycles).

(C) Upper panel: RUNX3 displaces TCF4 from TCF binding sites of the *cyclin D1* and c-*Myc* promoters in a dose-dependent manner. A DLD1 stable transfectant in the lower panel was subjected to ChIP assay with the indicated antibodies and number of PCR cycles. Lower panel: western blot analysis of RUNX3 induction in DLD1 stably transfected with inducible *RUNX3* following stimulation with 20 μM ponasterone A (Pon A).

(D) Quantification by real-time PCR of ChIP assay for TCF4 and β-catenin occupancy at TCF consensus sites of the *cyclin D1* (white bars) and c-*Myc* (gray bars) promoters. Relative occupancy in the RUNX3-expressing DLD1 clone was compared to that in the control clone (see [E]). TCF4 binding in HCT116 clones in which RUNX3 was knocked down (AS-Cl.1 and AS-Cl.2) was compared to that in the control clone (see [E]). Relative extent of PCR amplification of ChIP using negative control primer sets (designed for the *cyclin D1* and c-*Myc* promoters) that do not flank any TCF consensus sites was less than 0.0001 in all trials.

(E) Protein expression profile in DLD1 clones transfected with vector (control) or FLAG-RUNX3 (RUNX3) and in HCT116 clones expressing control vector (control) or antisense *RUNX3* DNA (AS-Cl.1 and AS-Cl.2), as detected by western blot analysis.

(F) Left panel: real-time PCR quantification of *AXIN2*, *CD44*, and *DKK1* mRNA in DLD1 cells with inducible *RUNX3* expression. The amount of mRNA 24 hr after induction by Pon A was normalized against noninduced samples. Right panel: the amount of mRNA of the same set of genes in HCT116 cells in which RUNX3 was knocked down (average of AS-Cl.1 and AS-Cl.2; see [E]) was normalized to the control clone.

(G) TOPflash versus FOPflash activity (in arbitrary units) for control DLD1 cells (white bars) and DLD1 cells expressing RUNX3 (black bars; see [E]), and for control HCT116 cells (black bars) and HCT116 cells in which RUNX3 was knocked down (white bars; see [E]).

(H) Differential effects of RUNX3 knockdown in HCT116, SW620, COLO320, SW480, and SW403 cells. Upper panel: western blot analysis showing RUNX3 expression in cells treated with three independent RUNX3 shRNAs (sh1–3) and control shRNA. Lower panel: TOPflash/FOPflash activity in cells after RUNX3 knockdown was normalized to that of the controls.

Error bars represent SEM in (D), (F), and (G).

β-catenin/TCF4 to the TCF binding site in a dose-dependent manner (Figure S3A). Conversely, RUNX3 lost affinity for the RUNX site when bound to β-catenin/TCF4 (Figure S3C). These results suggest that RUNX3 and TCF4 mutually inhibit their respective DNA-binding activities through interactions involving their DNA-binding domains.

Adenomatous Polyps and Adenocarcinomas Are Induced in Intestine of *Runx3*^{+/−} and *Runx3*^{+/−} *Apc*[Min/+] Mice, Respectively

Since Wnt signaling is a well-known oncogenic pathway and RUNX3 is a nuclear effector of the well-established TGF-β tumor suppressor pathway, an intriguing possibility is that oncogenicity in intestinal epithelial cells reflects the relative activities of these two antagonistic pathways. The gastrointestinal tract epithelium of *Runx3*^{+/−} mice was indistinguishable from that of *Runx3*^{+/+} mice over a 1 year observation period. However, at around 65 weeks of age, small adenomas developed in the small intestine of *Runx3*^{+/−} mice at a frequency comparable to that of *Apc*[Min/+] mice on the same BALB/c background (54% of *Runx3*^{+/−} mice and 64% of *Apc*[Min/+] mice at 65 weeks; Figures 4A and 4B). All intestinal tumors obtained from *Runx3*^{+/−} (n = 54) and *Apc*[Min/+] (n = 22) mice were adenomatous polyps. Adenomatous polyps were also found in small intestine of *Runx3*^{+/−} mice on other genetic backgrounds, such as C3H/HeJ, at 65 weeks of age (55% of *Runx3*^{+/−} mice [6 of 11] developed 2.2 ± 0.9 tumors).

Loss of heterozygosity (LOH) of *Apc*, indicating biallelic inactivation of the gene, occurs frequently in adenomatous polyps of *Apc*[Min/+] mice (Polakis, 2000). Similarly, we found LOH of *Apc* in adenomatous polyps of *Apc*[Min/+] mice in this study (Figure S4B). In the case of adenomatous polyps of *Runx3*^{+/−} mice, downregulation of Runx3 expression was observed (Figures 5A and 5C), but LOH of *Runx3* was not detected (Figure S4A). Instead, we detected CpG island methylation of the *Runx3* promoter (Guo et al., 2002), suggesting that *Runx3* promoter methylation is one of the causes of Runx3 repression in adenoma cells (Figure S4C).

Adenomatous polyps found in both *Runx3*^{+/−} and *Apc*[Min/+] small intestines displayed upregulation of cyclin D1 and c-Myc (Figures 5A, 5C, and 5D) and downregulation of *p21* (Figures 5C and 5D), which is consistent with an earlier report that p21 can be repressed by β-catenin/TCF4 (van de Wetering et al., 2002). In both types of tumors, binding of β-catenin/Tcfs to the Tcf consensus sites in the *cyclin D1* and *c-Myc* promoters was enhanced despite the fact that obvious nuclear accumulation of β-catenin was observed only in *Apc*[Min/+] mice (Figures 5E–5G). These results indicate that the nuclear accumulation of oncogenic β-catenin in *Apc*[Min/+] mice and the downregulation of Runx3 in *Runx3*^{+/−} mice induce common phenotypes in our experimental system. To confirm that the tumorigenicity of cells deficient in *Runx3* activity is dependent on the activity of β-catenin/Tcf4, we used *Runx3*^{−/−} FID and FIL cells. Only *Runx3*^{−/−} FID and FIL cells, but not *Runx3*^{+/+} cells, formed tumors in inoculated mice (Figure S9C). *Runx3*^{−/−} FID and FIL cells stably expressing a dominant-negative form of TCF4 (van de Wetering et al., 2002) showed that the tumorigenicity of *Runx3*^{−/−} FID and FIL cells was indeed attenuated by inhibition of β-catenin/Tcf4 (Figure S9D).

Since RUNX3 and β-catenin/TCF4 antagonize each other, inactivation of *Runx3* in *Apc*[Min/+] mice should enhance intestinal carcinogenesis. In *Runx3*^{+/−} and *Apc*[Min/+] mice, adenomatous polyps (0.2 mm or larger in diameter) were induced in the small intestine, but not in the large intestine. In *Runx3*^{+/−}*Apc*[Min/+] mice, on the other hand, invasive adenocarcinomas (generally larger than 5 mm in diameter; Figures 4A and 4D) and adenomatous polyps were seen in the small and large intestines,
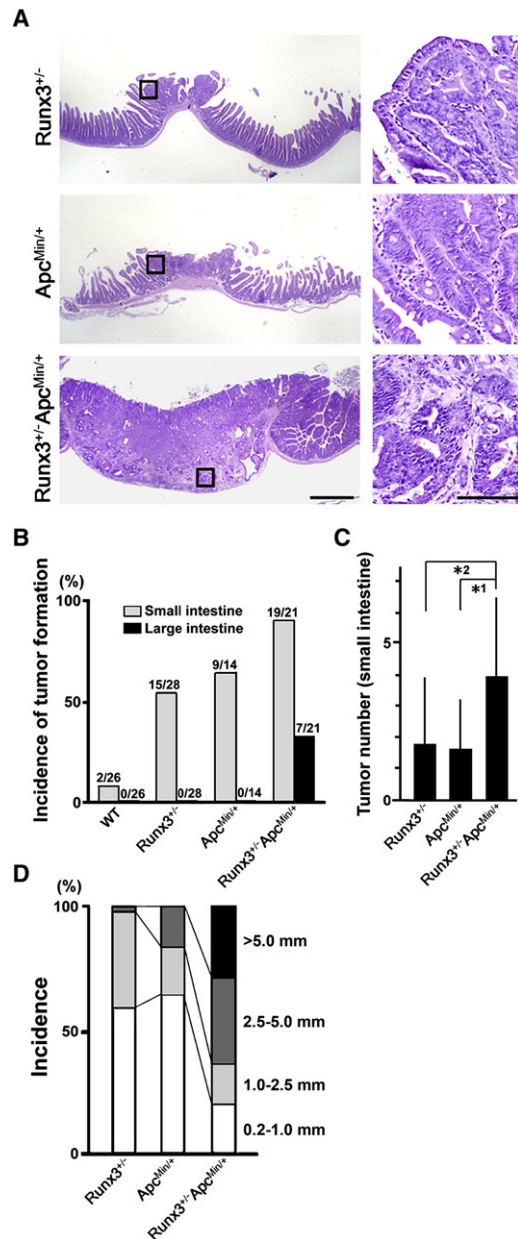

Figure 4. Adenomatous Polyps in Small Intestine of *Runx3*^{+/−} and *Apc*[Min/+] BALB/c Mice and Progression to Adenocarcinoma in *Runx3*^{+/−}*Apc*[Min/+] Mice

(A) H&E staining of tumors in small intestine of *Runx3*^{+/−}, *Apc*[Min/+], and *Runx3*^{+/−}*Apc*[Min/+] mice at 65 weeks of age. *Runx3*^{+/−}*Apc*[Min/+] mice developed adenocarcinomas. Boxed regions are enlarged at right. Scale bars = 1 mm (left) and 100 μm (right).

(B) Frequency of tumor formation in small and large intestines of mice of the indicated genotypes at 65 weeks of age. Tumors > 0.2 mm in diameter were counted.

(C) Number of tumors in small intestines of individual mice of the indicated genotypes at 65 weeks of age. Error bars represent SEM. *[1]p < 0.01; *[2]p < 0.05.

(D) Size distribution of polyps in small intestines of mice of the indicated genotypes at 65 weeks of age. Size classes indicate tumor diameter.
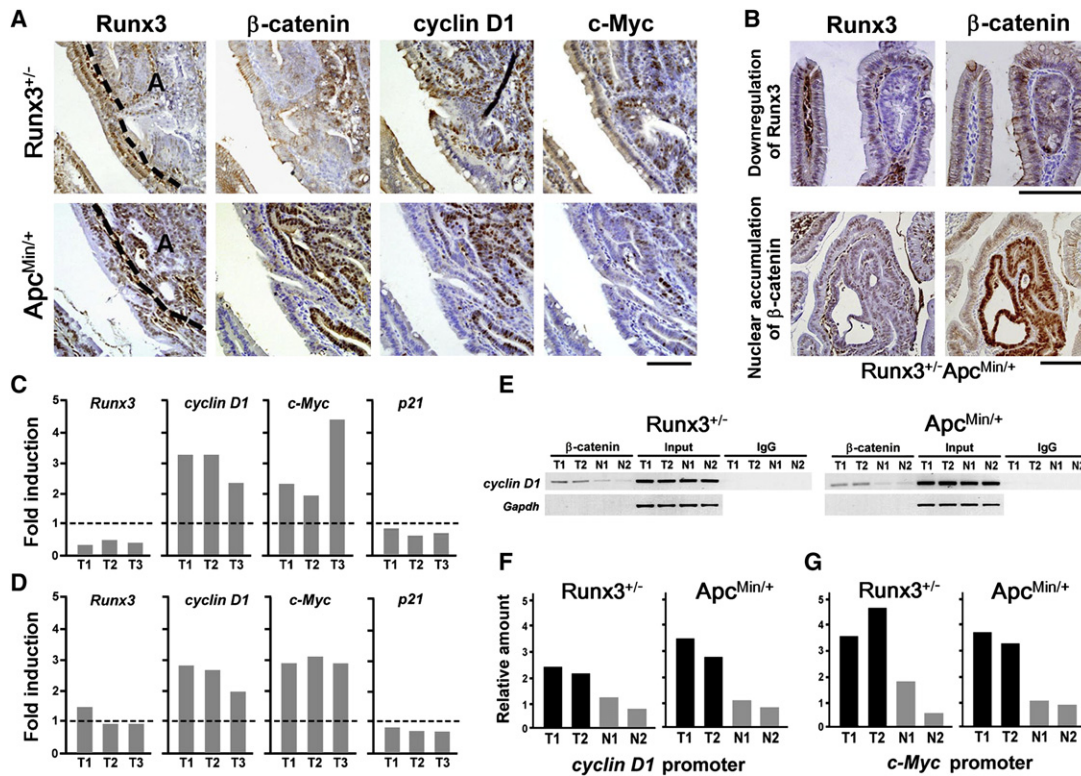
Figure 5. Adenomatous Polyps in Small Intestine of _Runx3_^{+/−} BALB/c Mice Displaying Downregulated Runx3 and Upregulated Cyclin D1 and c-Myc

(A) Immunodetection of Runx3, β-catenin, cyclin D1, and c-Myc in adenomatous polyps formed in the small intestine of $Runx3^{+/-}$ and $Apc^{Min/+}$ mice at 65 weeks of age. Dashed lines indicate the border between normal and adenomatous cells (marked "A").

(B) Very small adenomas formed in the jejunum of $Runx3^{+/-}Apc^{Min/+}$ mice were analyzed. When Runx3 was downregulated, β-catenin was not activated (upper panels). In contrast, when β-catenin was activated, Runx3 was not downregulated (lower panels).

Specimens were counterstained with hematoxylin in (A) and (B). Scale bars = 100 μm in (A) and (B).

(C and D) Quantification by real-time PCR of _Runx3_, _cyclin D1_, c-_Myc_, and _p21_ mRNA in individual polyps (T1–3) in $Runx3^{+/-}$ (C) and $Apc^{Min/+}$ (D) small intestines, normalized to the values of adjacent normal epithelium.

(E) Enhanced binding of β-catenin/Tcfs to the Tcf consensus site of the _cyclin D1_ promoter, as revealed by ChIP assay in polyps (T1 and T2) and adjacent normal tissues (N1 and N2) of $Runx3^{+/-}$ and $Apc^{Min/+}$ small intestines. T1 and T2 represent two pools of 3–4 polyps each from 1–2 mice with adenomas used for the ChIP assay. DNA fragments precipitated by anti-β-catenin antibody or control IgG were amplified by PCR (33 cycles). The _Gapdh_ promoter region was amplified as a negative control.

(F and G) Real-time PCR quantification of ChIP to measure bound β-catenin/Tcfs at Tcf consensus sites of the _cyclin D1_ (F) and c-_Myc_ (G) promoters, normalized to the inputs.

respectively (33.3% of 21 mice, 1–2 tumors per mouse; Figure 4B), at 65 weeks of age. Frequency of tumor formation, number of tumors per mouse, and tumor size were all increased in the small intestine of $Runx3^{+/-}Apc^{Min/+}$ mice (Figures 4B–4D).

An examination of the very small adenomas from $Runx3^{+/-}$ $Apc^{Min/+}$ mice showed either nuclear accumulation of β-catenin or loss of _Runx3_ expression, but not both (Figure 5B). This result is consistent with the hypothesis that the adenomas were induced by biallelic inactivation of either _Apc_ or _Runx3_. This observation explains why the number of tumors in $Runx3^{+/-}$ $Apc^{Min/+}$ small intestine was nearly equal to the sum of the tumors in $Apc^{Min/+}$ and $Runx3^{+/-}$ mice (Figure 4C). When the large adenomas or adenocarcinomas of the $Runx3^{+/-}Apc^{Min/+}$ mice were examined, β-catenin accumulation was observed in most cases, suggesting that alterations in both genes result in stronger activation of the Wnt pathway.

The extent of intestinal tumorigenicity conferred by the $Apc^{+/-}$ genotype varies in different mouse strains, with a higher incidence in C57BL/6 than in others (Shoemaker et al., 1997). We examined the effect of the C57BL/6 genetic background on the tumorigenicity of $Runx3^{+/-}$ and $Apc^{Min/+}$ using the F1 mice from the BALB/c × C57BL/6 cross. Although the tumorigenicity of $Apc^{Min/+}$ mice was strongly enhanced as expected, no tumors were observed in $Runx3^{+/-}$ mice within the 25 week observation period after birth (Figure S5A), and the numbers of tumors in the intestines of $Apc^{Min/+}$ and $Runx3^{+/-}Apc^{Min/+}$ mice were comparable at about 25 weeks of age (Figure S5B). Nevertheless, $Runx3^{+/-}$ status significantly promoted $Apc^{Min/+}$ tumorigenicity, as the size of small intestinal tumors and the frequency of large intestinal tumors were enhanced in $Runx3^{+/-}Apc^{Min/+}$ mice on the BALB/c × C57BL/6 background (Figures S5A, S5C, and S5D).
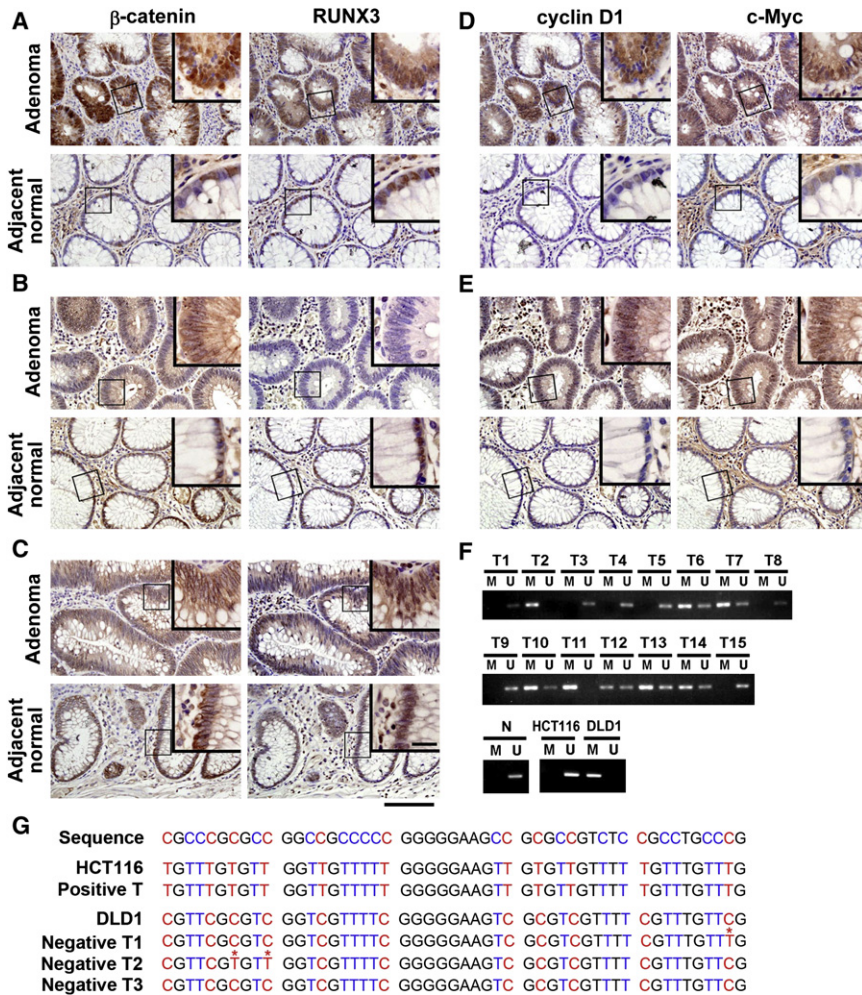
Figure 6. Downregulation of RUNX3 Expression without Nuclear Accumulation of β-Catenin in Human Adenomatous Polyps

(A–C) Three patterns of β-catenin and RUNX3 expression in 35 human cases: type A, nuclear β-catenin with RUNX3 in nuclei (A); type B, membranous β-catenin without RUNX3 expression (B); and type C, membranous β-catenin with RUNX3 expression (C). Images in (A), (B), and (C) show cases T4, T6, and T9 in (F), respectively. Enlargement of part of (A)–(C) is shown in Figure S6.

(D and E) Upregulation of cyclin D1 and c-Myc in adenomas of type A (D) and type B (E).

Four slides each of adenomas and adjacent normal epithelium shown in (A) and (D) (type A) and in (B) and (E) (type B) are all serial sections. Regions indicated by boxes in larger images are magnified in the insets. Specimens were counterstained with hematoxylin. Scale bars = 100 μm in larger images and 20 μm in insets.

(F) Methylation-specific PCR (MSP) analysis of the *RUNX3* promoter in normal human colon epithelium and DLD1 and HCT116 cells. Data are representative of 15 (T1–15) of a total of 35 human adenomatous polyps (see Table S1).

(G) Methylation status of the CpG dinucleotide between −70 and −21 relative to the translation initiation site of the *RUNX3* exon 1 region. The nucleotide sequence (sense strand) of the MSP products from RUNX3-positive and -negative tumors and DLD1 and HCT116 cells are shown. A red C indicates resistance to bisulfite treatment due to methylation. Unmethylated C (indicated in blue) was converted to T by bisulfite treatment. An asterisk above a T indicates an unmethylated C residue in RUNX3-negative tumors.

RUNX3 Is Frequently Downregulated in Human Colon Adenomatous Polyps without Apparent Accumulation of β-Catenin

We next examined RUNX3 expression and β-catenin accumulation in sporadic human colon adenomatous polyps. Ten of thirty-five cases (29%) tested showed reduced RUNX3 without apparent nuclear/cytoplasmic accumulation of β-catenin ("type B"; Figure 6B and Figure S6B), while 15 of 35 cases (43%) showed accumulation of β-catenin without inactivation of RUNX3 ("type A"; Figure 6A and Figure S6A). The remaining cases showed membranous β-catenin without inactivation of RUNX3 ("type C"; Figure 6C and Figure S6C). In both A and B types of adenomas, upregulation of cyclin D1 and c-Myc was observed consistently (Figures 6D and 6E). Cyclin D1 and c-Myc were upregulated in 100% (13/13) and 92% (12/13), respectively, of type A polyps and 80% (8/10) and 100% (10/10), respectively, of type B polyps. Another target gene of canonical Wnt signaling, CD44, was also upregulated in 100% (10/10) of both A and B types (Figures S7A and S7B). In type C polyps, on the other hand, cyclin D1, c-Myc, and CD44 were upregulated in 67% (6/9), 67% (6/9), and 86% (6/7) of cases, respectively (data not shown). Therefore, Wnt target genes are upregulated in two-thirds or more of type C cases, suggesting that there might be another activation mechanism of Wnt signaling.

In agreement with the mouse cases, methylation of the *RUNX3* promoter region was detected in all cases that showed downregulation of RUNX3 (Figures 6F and 6G; Table S1). We frequently observed the unmethylated allele in addition to the methylated allele (Figure 6F). This is likely because small tumors that we analyzed were inadvertently contaminated with normal surrounding tissue wherein the *RUNX3* promoter was unmethylated. Methylation was also detected in some adenomas that expressed RUNX3 (Table S1). This is probably due to partial methylation of the promoter region. It is likely that *RUNX3* is biallelically inactivated in human colon adenomatous polyps in which RUNX3 expression is lost without β-catenin accumulation (type B), since monoallelic inactivation of *Runx3* per se does not eliminate the expression of Runx3 in mice.

RUNX3 Is Frequently Inactivated in Human Colorectal Cancers Showing Concomitant Accumulation of β-Catenin

As colon adenomas do not always progress to carcinomas (Kinzler and Vogelstein, 1996), we examined whether RUNX3 is inactivated in colon carcinomas. Consistent with earlier reports by others (Kinzler and Vogelstein, 1996; Bodmer, 2006), nuclear/cytoplasmic accumulation of β-catenin was observed in 45 of 48 specimens tested (94%) (Figures 7A–7C; Table S2). On the other
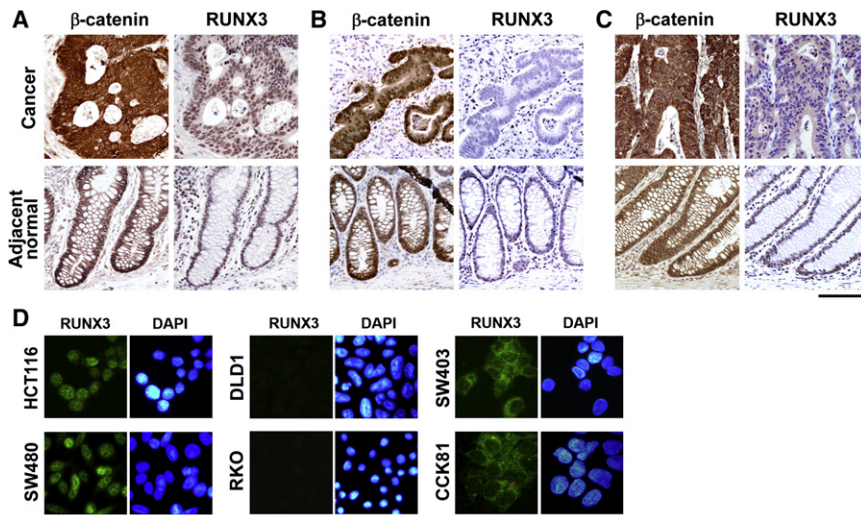
Figure 7. RUNX3 Inactivation by Gene Silencing and Protein Mislocalization with Concomitant Accumulation of β-Catenin in Human Colorectal Cancers

(A–C) Differential staining patterns of RUNX3 in human colorectal cancers. Positive (A), negative (B), and cytoplasmic positive (C) are summarized as "P," "N," and "C," respectively, in Table S2. Specimens were counterstained with hematoxylin.

(D) Differential staining patterns of RUNX3 in human colorectal cancer cell lines: positive (HCT116 and SW480), negative (DLD1 and RKO), and cytoplasmic positive (SW403 and CCK81).

Scale bars = 100 μm in (A)–(C) and 50 μm in (D).

hand, RUNX3 was found to be reduced in 14 of 48 cases (29%) (Figure 7B; "N" in Table S2) and localized in cytoplasm, an alternative mechanism of RUNX3 inactivation (Ito et al., 2005), in 7 of 48 cases (15%) (Figure 7C; "C" in Table S2). RUNX3 was therefore inactive in at least 44% of colon cancers, most of which showed nuclear/cytoplasmic accumulation of β-catenin (Table S2). This was in contrast to human colon adenomas, none of which showed simultaneous nuclear/cytoplasmic accumulation of β-catenin and RUNX3 inactivation (Figure 6). RUNX3 inactivation is also prevalent in human colorectal cancer cell lines. RUNX3 was undetectable in 14 of 22 human colorectal cancer cell lines (Figure 2A), was excluded from the nucleus in SW403 and CCK81 cell lines (Figure 7D), and did not interact with TCF4 in the SW480 cell line. The growth-inhibitory and tumor-suppressive effects of RUNX3 in the human colorectal cancer cell lines DLD1 (*RUNX3*-negative) and HCT116 (*RUNX3*-positive), both of which are β-catenin-activated cell lines, were confirmed by the exogenous expression of RUNX3 and knockdown of RUNX3, respectively (Figures S9A and S9B).

It was previously reported that Runx3 was not expressed in intestinal epithelial cells and that the intestinal hyperplasia observed in *Runx3*⁻/⁻ mice was due to inflammation caused by loss of *Runx3* function in leukocytic populations (Brenner et al., 2004). However, we observed only a few small foci of inflammation in colon epithelium of our *Runx3*⁻/⁻ mice (Figure S1A). Inflammation is therefore unlikely to cause hyperplastic changes in *Runx3*⁻/⁻ intestine. We used two approaches to further confirm that the loss of *Runx3* function in intestinal epithelial cells is responsible for their tumorigenic potential. In the first approach, we generated mice whose leukocytes but not epithelial cells were *Runx3*⁻/⁻ by transplanting bone marrow cells of *Runx3*⁻/⁻ mice into irradiated wild-type mice. Histological examination of the small and large intestines of these mice 1 year after transplantation revealed neither hyperplasia nor dysplasia (Figures S8A–S8E). In the second approach, we compared the tumorigenicity of *Runx3*⁺/⁺ and *Runx3*⁻/⁻ FID and FIL cells in nude mice. As mentioned earlier and as shown in Figure S9C, only *Runx3*⁻/⁻ cells formed tumors. These results indicate that the tumorigenicity of intestinal epithelial cells of *Runx3*⁻/⁻ mice is epithelial cell autonomous. Our results do not, however, exclude the possibility that leukocytes or other mesenchymal cells may affect the growth of epithelial cells when the intestinal epithelium is encompassed by these cells, as reported for *Smad4*-deficient mice (Kim et al., 2006; Pan et al., 2007).

DISCUSSION

Our results show that inactivation of either RUNX3 or APC can induce intestinal adenomas in humans and mice. However, inactivation of both RUNX3 and APC appears to provide a more favorable condition for the progression of these adenomas to adenocarcinomas.

The results presented here suggest that RUNX3 modulates the strength of activated Wnt signaling, either physiologically by Wnt ligands or pathologically by APC inactivation or β-catenin activation, through interaction with the β-catenin/TCF4 complex. In the absence of Wnt ligand stimulation, RUNX3 inactivation will not affect TCF4 and β-catenin protein levels or result in aberrant Wnt pathway activity. Without RUNX3, the β-catenin/TCF4 transcriptional activity resulting from normal Wnt ligand activation is enhanced or prolonged, or both, owing to the absence of RUNX3-mediated repression. Even when the Wnt pathway is aberrantly activated due to APC inactivation or β-catenin activation, the signal output may still be restrained by RUNX3. Concomitant inactivation of APC, or activation of β-catenin, and inactivation of RUNX3 would result in ligand-independent and unconstrained Wnt pathway signaling that favors the progression of intestinal tumors.

Of the five RUNX3-positive human colon cancer cell lines tested, knockdown of RUNX3 in the SW480 and SW403 cell lines did not result in a significant increase in β-catenin/TCF4 transcriptional activity, which can be attributed to the lack of interaction between RUNX3 and TCF4 in SW480 cells and protein mislocalization in SW403 cells (Figure 3H). This result emphasizes the importance of the interaction between RUNX3 and TCF4 for attenuation of Wnt signaling by RUNX3. Preliminary results suggest that RUNX3-TCF4 interaction is regulated by a signaling pathway that appears to be defective in SW480 cells. Therefore, it is possible that RUNX3 may be inactive in certain colon cancers even when it is expressed and properly localized in nuclei.

When adenomatous polyps were induced in *Runx3*^{+/−} intestine, the remaining intact *Runx3* allele was silenced in the majority of the polyps as judged by *Runx3* promoter methylation. This suggests that inactivation of *Runx3* occurs at an early stage of carcinogenesis. CpG island methylator phenotype (CIMP) has been proposed as a mechanism for sporadic colorectal cancer (Toyota et al., 1999). As many as 35%–40% of colorectal cancers have been classified as CIMP (Goel et al., 2007), and RUNX3 is one of five markers used to classify CIMP+ tumors (Weisenberger et al., 2006).

Transgenic *Apc*[Min/+] mice overexpressing the DNA methyltransferase Dnmt3b show increased tumorigenesis (Linhart et al., 2007). In the tumors of these mice, the tumor suppressor genes *Sfrp2*, *Sfrp4*, and *Sfrp5* are methylated and silenced, whereas *Mlh1*, *Mgmt*, *Cdkn2b*, *Apc*, *Rb1*, *Vhlh*, and *Brca1*, genes often methylated in cancer cells, are not. Given that Linhart et al. also noted reduced *Runx3* expression in the tumors of these mice, our conclusion that Runx3 is a downstream attenuator of Wnt signaling cascade seems plausible. Whether *Runx3* is a target of Dnmt3b during the early stages of carcinogenesis remains to be determined.

Somewhat surprisingly, *Runx3*^{−/−} mice did not develop epithelial tumors, unlike *Runx3*^{+/−} mice. As homozygous mutant mice typically die at around 10 months of age, it may be that they die before tumors can form. However, this might not be the only explanation. In studies of acute myeloid leukemia, it has been shown that homozygous inactivation of the transcription factors PU.1, C/EBPα, or GATA-1 hardly induces leukemia, whereas a strong association is observed between leukemogenesis and hypomorphic alleles of these transcription factors, suggesting that a threshold level of gene expression is required for carcinogenesis (reviewed by Rosenbauer et al., 2005). This might be the case as well in *Runx3*^{+/−} mice.

Gut development and intestinal stem cell maintenance and differentiation are regulated by interactions between key signaling pathways. Since β-catenin and TCF4 are downstream effectors of the canonical Wnt signaling pathway and RUNX3 is a nuclear effector of the TGF-β superfamily, our results suggest that proliferation signals transmitted by the Wnt pathway and antiproliferation signals transmitted by the TGF-β family pathway culminate in the ternary complex formed by β-catenin/TCF4 and RUNX3. The ternary complex would function to harmoniously coregulate gut development and maintain the normal proliferative state of the gut epithelium. In this study, we showed that a DNA-binding-negative mutant of RUNX3 can attenuate β-catenin/TCF4 activity, indicating that RUNX3 can act independently of its transcription factor activity. Judging from the data presented here, its activity as an attenuator of the Wnt signaling pathway would have a profound role in gut development, homeostasis, and cancer. The observations made here provide insight into the interaction between the Wnt and TGF-β superfamily pathways in intestinal tumorigenesis. How this interaction is further regulated by interactions with other signaling pathways is currently under investigation.

EXPERIMENTAL PROCEDURES

Cell Lines, Mouse Lines, and RUNX3 shRNAs

Colorectal cancer cells were maintained in DMEM supplemented with 10% fetal bovine serum. Transfections with pcDNA3, pcDNA-FLAG-RUNX3, or pEF-BOS-neo-RUNX3-AS were performed as described previously (Ito et al., 2005). Stable transfectants were selected using 0.5 mg/ml G418 (GIBCO). An ecdysone-inducible FLAG-RUNX3 clone of DLD1 was prepared as described previously (Yamamura et al., 2006). shRNAs targeting RUNX3 (sh1, 5′-GCCCAGAGAAGATGAGTCTAT-3′; sh2, 5′-AAGCAGCTATGAATC CATTGT-3′; sh3, 5′-TCAGTAGTGGGTACCAATCTT-3′) and control shRNA were obtained from SuperArray Bioscience. pGeneClip-hMGFP (Promega) was used as the vector for transfection. Sorted cells showing GFP expression were subjected to western blot analysis and transfected with the reporter plasmids TOPflash and FOPflash (Upstate).

Immunocytochemistry to detect RUNX3 in colorectal cancer cell lines was performed using anti-RUNX3 antibody (MBL R3-6E9; Ito et al., 2005).

Mouse small and large intestinal epithelial cell lines FID and FIL, respectively, were established from isolated intestinal epithelium of 16.5 dpc *Runx3*^{+/+}*p53*^{−/−} and *Runx3*^{−/−}*p53*^{−/−} fetuses on the C57BL/6 background and maintained as described previously for similarly obtained mouse gastric epithelial cell lines (Li et al., 2002).

To generate *Runx3*-deficient and *Apc*[Min/+] mice on the BALB/c background, male *Runx3*^{+/−} mice on the C57BL/6 background (Li et al., 2002) and C57BL/6[Min/+] mice (The Jackson Laboratory) were backcrossed with wild-type BALB/c female mice for at least six generations. Animal studies were approved by the Institutional Animal Care and Use Committee of the National University of Singapore (protocol numbers 752/05 and 857/05).

Histological Analysis

Tissues were fixed with 10% formalin (for human tissues) or 4% paraformaldehyde (for mouse tissues), embedded in paraffin, and sectioned (5 μm). Anti-RUNX3 (MBL R3-1E10 for mouse; Yano et al., 2006; MBL R3-6E9 for human; Ito et al., 2005), anti-Ki67 (DAKO M7249), anti-c-Myc (Santa Cruz sc-764 for mouse; Upstate 06-340 for human), anti-EphrinB1 (Santa Cruz sc-910), anti-EphB2 (R&D Systems AF467), anti-lysozyme (DAKO A0099), anti-cyclin D1 (Zymed 13-4500 for mouse; Novocastra NCL-CYCLIN D1-GM for human), and anti-β-catenin (Santa Cruz sc-7199) antibodies were used on rehydrated sections pretreated with Target Retrieval Solution (DAKO). An EnVision+ system (HRP/DAB) (DAKO) was used for visualization. BrdU incorporation and cellular proliferation were detected with a BrdU Labeling and Detection Kit II (Roche).

Human Polyps and Cancers

All polyps tested were adenomas resected during colonoscopic examination in the context of regular screening and were made up of approximately similar proportions of left- and right-sided adenomas. The carcinomas were surgically resected. None of the patients with adenomas or carcinomas had a clinical presentation (including family history) reminiscent of inherited carcinoma or histological features suggesting an inherited pattern. Indeed, from both clinical and pathological viewpoints, the adenomas and carcinomas were sporadic in nature. Furthermore, the patients had no other predisposing factors and, in particular, no inflammatory bowel disease. The human tissue samples in this study were analyzed with prior approval from the institutional ethics committee of the National University of Singapore (NUS-IRB reference number 06-178).

Western Blot Analysis and Immunoprecipitation

Lysates prepared from colorectal cancer cell lines and mouse intestinal tissues containing 30 μg of proteins were analyzed by western blot using anti-RUNX3 (MBL R3-5G4; Ito et al., 2005), anti-dephosphorylated β-catenin (Alexis ALX-804-260 for human; Upstate 05-665 for mouse), anti-TCF4 (Upstate 05-511), anti-CD44 (Endogen MA-4405), anti-c-Myc (Santa Cruz sc-40 for human; Santa Cruz sc-764 for mouse), anti-cyclin D1 (BD Biosciences 556470), anti-conductin (Santa Cruz sc-8570), anti-EphrinB1 (R&D Systems AF473), anti-EphB2 (R&D Systems AF467), and anti-β-actin (Sigma A5441) antibodies.

Whole-cell extracts of HCT116 or 293T cells expressing 6×Myc-TCF4, FLAG-RUNX3, FLAG-RUNX3(R178Q) (Inoue et al., 2007), HA-β-catenin, β-catenin (WT), β-catenin (Δ45; Morin et al., 1997), or β-catenin (S33Y; Morin et al., 1997) were immunoprecipitated with anti-Myc (Santa Cruz sc-789), anti-HA (Santa Cruz sc-805), and anti-β-catenin (BD Biosciences 610153) antibodies or anti-FLAG M2 agarose (Sigma A2220), followed by western blot analysis using anti-Myc (Santa Cruz sc-40), anti-HA (Santa Cruz sc-7392), anti-β-catenin (BD Biosciences 610153), or anti-FLAG (Sigma F7429) antibodies. For

two-step coimmunoprecipitation, 3×FLAG peptide (Sigma F4799) was used to elute proteins from anti-FLAG M2 agarose.

To detect endogenous protein interactions, nuclear extracts were prepared using NE-PER Nuclear and Cytoplasmic Extraction Reagents (Pierce) and treated with DNase I (Promega). Immunoprecipitation was performed using anti-RUNX3 (MBL R3-5G4), anti-TCF4 (Upstate 05-511), or anti-dephosphorylated β-catenin (Alexis ALX-804-260) antibodies or mouse normal IgG, followed by western blot analysis.

HA-β-catenin, 6×Myc-TCF4, and 6×His-RUNX3 were translated in vitro using the TNT T7 Quick Coupled Transcription/Translation System (Promega L1170). Proteins pulled down by Ni-NTA agarose (QIAGEN 30210) were revealed by western blot analysis using anti-HA (Santa Cruz sc-7392), anti-Myc (Santa Cruz sc-40), and anti-His (Clontech 631212) antibodies.

Reporter Assay

The mutant *cyclin D1* promoter construct (CyclinD1-mTCF) was made by mutating the TCF consensus sequence located near the nucleotide −80 (from CTTTG<u>ATC</u> to CTTTG<u>GCC</u>) in D1Δ-944pXP2 (CyclinD1-WT; Herber et al., 1994) using a QuikChange XL Site-Directed Mutagenesis Kit (Stratagene). DLD1 cells were transfected with reporter plasmids; TOP/FOPflash (Upstate), CyclinD1-WT, or CyclinD1-mTCF along with pRL-TK (Promega) and effector plasmids; pcDNA3, pcDNA-FLAG-RUNX3, or pcDNA-FLAG-RUNX3(R178Q) using FuGENE 6 (Roche). Luciferase activity was measured using the Dual-Luciferase Reporter Assay System (Promega) and normalized to luciferase activity expressed by pRL-TK. To examine the β-catenin/Tcf-dependent reporter activities in response to Wnt3a stimulation, FID cells were transfected with TOP/FOPflash and treated with conditioned media collected from Wnt3a-expressing or parental L cell cultures (Shibamoto et al., 1998) for 24 hr.

Chromatin Immunoprecipitation

Chromatin immunoprecipitation (ChIP) was performed using a Chromatin Immunoprecipitation Assay Kit (Upstate) and anti-TCF4 (Santa Cruz sc-13027) and anti-dephosphorylated β-catenin (Alexis ALX-804-260) antibodies or mouse normal IgG. Primers used to amplify DNA fragments containing the TCF consensus site were 5′-AGGCGCGGCGGCTCAGGGATG-3′ and 5′-ACTCTGCTGCTCGCTGCTACT-3′ for the human *cyclin D1* promoter (Nateri et al., 2005), 5′-TTGCTGGGTTATTTTAATCAT-3′ and 5′-ACTGTTTGACAAACCGCATCC-3′ for the human c-*Myc* promoter (Nateri et al., 2005), 5′-CCTCCCCCTTTTCTCTGCCC-3′ and 5′-CCTCTGGAGGCTGCAGGACTTTGC-3′ for the murine *cyclin D1* promoter, and 5′-AATGCACAGCGTAGTATTCAGG-3′ and 5′-AAACCGTTAACCCCTTCCTCC-3′ for the murine c-*Myc* promoter. Primers used as negative controls were 5′-CGTCTTCACCACCATGGAGA-3′ and 5′-CGGCCATCACGCGACAGTTT-3′ for the human *GAPDH* gene (Nateri et al., 2005) and 5′-GGGGTTGCTGTGTCACTACCG-3′ and 5′-CAGAGACCTGAATGCTGCTTCC-3′ for the murine *Gapdh* gene.

Quantitative PCR for ChIP was performed using a SYBR Green PCR Kit (QIAGEN) and a 7500 Fast Real-Time PCR System (Applied Biosystems). The following primers were used for quantitative PCR amplification of regions of human gene promoters containing the TCF consensus and no TCF site, respectively: 5′-CCCTCCCGCTCCCATTC-3′/5′-TACAGGGGAGTTTTGTTGAAGTTG-3′ and 5′-GCAGTCGCTGAGATTCTTTGG-3′/5′-AGAATGGGCGCATTTCCA-3′ for the *cyclin D1* promoter, and 5′-CCCGTCTAGCACCTTTGATTTC-3′/5′-TGTTGCAAACCGGCGC-3′ and 5′-CGGCAGCCCGAGACTGT-3′/5′-TCAGAAGAGACAAATCCCCTTTG-3′ for the c-*Myc* promoter.

Quantitative RT-PCR

Quantitative RT-PCR was performed using an RNeasy Kit (QIAGEN), Omniscript RT Kit (QIAGEN), 7500 Fast Real-Time PCR System (Applied Biosystems), and TaqMan Gene Expression Assays (Applied Biosystems; Hs00610344_m1 for human *AXIN2*; Hs00153304_m1 for human *CD44*; Hs00183740_m1 for human *DKK1*; Hs99999903_m1 for human β-*actin* for normalization; Mm00490666_m1 for murine *Runx3*; Mm00432359_m1 for murine *cyclin D1*; Mm00487803_m1 for murine c-*Myc*; Mm00432448_m1 for murine *p21*; Mm99999915_g1 for murine *Gapdh* for normalization).

Methylation-Specific PCR and Bisulfite Sequencing

Genomic DNA extracted by proteinase K digestion from rehydrated sections of human tissues or DLD1 and HCT116 cells was treated with sodium bisulfite

using a CpGenome DNA Modification Kit (Chemicon). PCR was performed using the primer sets 5′-ATAATAGCGGTCGTTAGGGCGTCG-3′ and 5′-GCTTCTACTTTCCCGCTTCTCGCG-3′ for methylated DNA and 5′-ATAATAGTGGTTGTTAGGGTGTTG-3′ and 5′-ACTTCTACTTTCCCACTTCTCACA-3′ for unmethylated DNA as described previously (Homma et al., 2006). The PCR products were subjected to sequencing.

Statistics

Statistical evaluation was performed by Student's unpaired t test or Mann-Whitney U test. Data are presented as mean ± SEM. $p < 0.05$ was considered statistically significant.

SUPPLEMENTAL DATA

The Supplemental Data include Supplemental Experimental Procedures, Supplemental References, nine figures, and two tables and can be found with this article online at http://www.cancercell.org/cgi/content/full/14/3/226/DC1/.

REFERENCES

Andreu, P., Colnot, S., Godard, C., Gad, S., Chafey, P., Niwa-Kawakita, M., Laurent-Puig, P., Kahn, A., Robine, S., Perret, C., et al. (2005). Crypt-restricted proliferation and commitment to the Paneth cell lineage following *Apc* loss in the mouse intestine. Development *132*, 1443–1451.

Batlle, E., Henderson, J.T., Beghtel, H., van den Born, M.M.W., Sancho, E., Huls, G., Meeldijk, J., Robertson, J., van de Wetering, M., Pawson, T., et al. (2002). β-catenin and TCF mediate cell positioning in the intestinal epithelium by controlling the expression of EphB/EphrinB. Cell *111*, 251–263.

Blyth, K., Cameron, E.R., and Neil, J.C. (2005). The RUNX genes: gain or loss of function in cancer. Nat. Rev. Cancer *5*, 376–387.

Bodmer, W.F. (2006). Cancer genetics: colorectal cancer as a model. J. Hum. Genet. *51*, 391–396.

Brenner, O., Levanon, D., Negreanu, V., Golubkov, O., Fainaru, O., Woolf, E., and Groner, Y. (2004). Loss of Runx3 function in leukocytes is associated with spontaneously developed colitis and gastric mucosal hyperplasia. Proc. Natl. Acad. Sci. USA *101*, 16016–16021.

Chi, X.Z., Yang, J.O., Lee, K.Y., Ito, K., Sakakura, C., Li, Q.L., Kim, H.R., Cha, E.J., Lee, Y.H., Kaneda, A., et al. (2005). RUNX3 suppresses gastric epithelial cell growth by inducing $p21^{WAF/Cip1}$ expression in cooperation with transforming growth factor β-activated SMAD. Mol. Cell. Biol. *25*, 8097–8107.

Derynck, R., Akhurst, R.J., and Balmain, A. (2001). TGF-β signaling in tumor suppression and cancer progression. Nat. Genet. *29*, 117–129.

Goel, A., Arnold, C.N., Tassone, P., Chang, D.K., Niedzwiecki, D., Dowell, J.M., Wasserman, L., Compton, C., Mayer, R.J., Bertagnolli, M.M., et al. (2004). Epigenetic inactivation of *RUNX3* in microsatellite unstable sporadic colon cancers. Int. J. Cancer *112*, 754–759.

Goel, A., Nagasaka, T., Arnold, C.N., Inoue, T., Hamilton, C., Niedzwiecki, D., Compton, C., Mayer, R.J., Goldberg, R., Bertagnolli, M.M., et al. (2007). The CpG island methylator phenotype and chromosomal instability are inversely correlated in sporadic colorectal cancer. Gastroenterology *132*, 127–138.

Guo, W.H., Weng, L.Q., Ito, K., Chen, L.F., Nakanishi, H., Tatematsu, M., and Ito, Y. (2002). Inhibition of growth of mouse gastric cancer cells by *Runx3*, a novel tumor suppressor. Oncogene *21*, 8351–8355.

He, T.-C., Sparks, A.B., Rago, C., Hermeking, H., Zawel, L., de Costa, L.T., Morin, P.J., Vogelstein, B., and Kinzler, K.W. (1998). Identification of c-*MYC* as a target of the APC pathway. Science *281*, 1509–1512.

Herber, B., Truss, M., Beato, M., and Müller, R. (1994). Inducible regulatory elements in the human cyclin D1 promoter. Oncogene *9*, 1295–1304.

Homma, N., Tamura, G., Honda, T., Matsumoto, Y., Nishizuka, S., Kawata, S., and Motoyama, T. (2006). Spreading of methylation within *RUNX3* CpG island in gastric cancer. Cancer Sci. *97*, 51–56.

Inoue, K., Ito, K., Osato, M., Lee, B., Bae, S.C., and Ito, Y. (2007). The transcription factor Runx3 represses the neurotrophin receptor TrkB during lineage commitment of dorsal root ganglion neurons. J. Biol. Chem. *282*, 24175–24184.

Ito, K., Liu, Q., Salto-Tellez, M., Yano, T., Tada, K., Ida, H., Huang, C., Shah, N., Inoue, M., Rajnakova, A., et al. (2005). RUNX3, a novel tumor suppressor, is frequently inactivated in gastric cancer by protein mislocalization. Cancer Res. *65*, 7743–7750.

Ito, Y. (2008). RUNX genes in development and cancer: regulation of viral gene expression and the discovery of RUNX family genes. Adv. Cancer Res. *99*, 33–76.

Jass, J.R., Whitehall, V.L.J., Young, J., and Leggett, B.A. (2002). Emerging concepts in colorectal neoplasia. Gastroenterology *123*, 862–876.

Kahler, R.A., and Westendorf, J.J. (2003). Lymphoid enhancer factor-1 and β-catenin inhibit Runx2-dependent transcriptional activation of the osteocalcin promoter. J. Biol. Chem. *278*, 11937–11944.

Kim, B.G., Li, C., Qiao, W., Mamura, M., Kasperczak, B., Anver, M., Wolfraim, L., Hong, S., Mushinski, E., Potter, M., et al. (2006). Smad4 signalling in T cells is required for suppression of gastrointestinal cancer. Nature *441*, 1015–1019.

Kinzler, K.W., and Vogelstein, B. (1996). Lessons from hereditary colorectal cancer. Cell *87*, 159–170.

Ku, J.L., Kang, S.B., Shin, Y.K., Kang, H.C., Hong, S.H., Kim, I.J., Shin, J.H., Han, I.O., and Park, J.G. (2004). Promoter hypermethylation downregulates *RUNX3* gene expression in colorectal cancer cell lines. Oncogene *23*, 6736–6742.

Li, Q.L., Ito, K., Sakakura, C., Fukamachi, H., Inoue, K., Chi, X.Z., Lee, K.Y., Nomura, S., Lee, C.W., Han, S.B., et al. (2002). Causal relationship between the loss of *RUNX3* expression and gastric cancer. Cell *109*, 113–124.

Lin, S.Y., Xia, W., Wang, J.C., Kwong, K.Y., Spohn, B., Wen, Y., Pestell, R.G., and Hung, M.C. (2000). β-catenin, a novel prognostic marker for breast cancer: its roles in cyclin D1 expression and cancer progression. Proc. Natl. Acad. Sci. USA *97*, 4262–4266.

Linhart, H.G., Lin, H., Yamada, Y., Moran, E., Steine, E.J., Gokhale, S., Lo, G., Cantu, E., Ehrich, M., He, T., et al. (2007). Dnmt3b promotes tumorigenesis in vivo by gene-specific de novo methylation and transcriptional silencing. Genes Dev. *21*, 3110–3122.

Mishra, L., Shetty, K., Tang, Y., Stuart, A., and Byers, S.W. (2005). The role of TGF-β and Wnt signaling in gastrointestinal stem cells and cancer. Oncogene *24*, 5775–5789.

Morin, P.J., Sparks, A.B., Korinek, V., Barker, N., Clevers, H., Vogelstein, B., and Kinzler, K.W. (1997). Activation of β-catenin-Tcf signaling in colon cancer by mutations in β-catenin or APC. Science *275*, 1787–1790.

Nateri, A.S., Spencer-Dene, B., and Behrens, A. (2005). Interaction of phosphorylated c-Jun with TCF4 regulates intestinal cancer development. Nature *437*, 281–285.

Pan, D., Schomber, T., Kalberer, C.P., Terracciano, L.M., Hafen, K., Krenger, W., Hao-Shen, H., Deng, C., and Skoda, R.C. (2007). Normal erythropoiesis but severe polyposis and bleeding anemia in *Smad4*-deficient mice. Blood *110*, 3049–3055.

Polakis, P. (2000). Wnt signaling and cancer. Genes Dev. *14*, 1837–1851.

Rosenbauer, F., Koschmieder, S., Steidl, U., and Tenen, D.G. (2005). Effect of transcription-factor concentrations on leukemic stem cells. Blood *106*, 1519–1524.

Sansom, O.J., Reed, K.R., Hayes, A.J., Ireland, H., Brinkmann, H., Newton, I.P., Batlle, E., Simon-Assmann, P., Clevers, H., Nathke, I.S., et al. (2004). Loss of Apc in vivo immediately perturbs Wnt signaling, differentiation, and migration. Genes Dev. *18*, 1385–1390.

Shibamoto, S., Higano, K., Takada, R., Ito, F., Takeichi, M., and Takada, S. (1998). Cytoskeletal reorganization by soluble Wnt-3a protein signaling. Genes Cells *3*, 659–670.

Shoemaker, A.R., Gould, K.A., Luongo, C., Moser, A.R., and Dove, W.F. (1997). Studies of neoplasia in the Min mouse. Biochim. Biophys. Acta *1332*, F25–F48.

Tetsu, O., and McCormick, F. (1999). β-catenin regulates expression of cyclin D1 in colon carcinoma cells. Nature *398*, 422–426.

Toyota, M., Ahuja, N., Ohe-Toyota, M., Herman, J.G., Baylin, S.B., and Issa, J.P.J. (1999). CpG island methylator phenotype in colorectal cancer. Proc. Natl. Acad. Sci. USA *96*, 8681–8686.

van de Wetering, M., Sancho, E., Verweij, C., de Lau, W., Oving, I., Hurlstone, A., van der Horn, K., Batlle, E., Coudreuse, D., Haramis, A.P., et al. (2002). The β-catenin/TCF-4 complex imposes a crypt progenitor phenotype on colorectal cancer cells. Cell *111*, 241–250.

van Es, J.H., Jay, P., Gregorieff, A., van Gijn, M.E., Jonkheer, S., Hatzis, P., Thiele, A., van den Born, M., Begthel, H., Brabletz, T., et al. (2005). Wnt signalling induces maturation of Paneth cells in intestinal crypts. Nat. Cell Biol. *7*, 381–386.

Weisenberger, D.J., Siegmund, K.D., Campan, M., Young, J., Long, T.I., Faasse, M.A., Hong Kang, G., Widschwendter, M., Weener, D., Buchanan, D., et al. (2006). CpG island methylator phenotype underlies sporadic microsatellite instability and is tightly associated with *BRAF* mutation in colorectal cancer. Nat. Genet. *38*, 787–793.

Yamamura, Y., Lee, W.L., Inoue, K., Ida, H., and Ito, Y. (2006). RUNX3 cooperates with FoxO3a to induce apoptosis in gastric cancer cells. J. Biol. Chem. *281*, 5267–5276.

Yano, T., Ito, K., Fukamachi, H., Chi, X.Z., Wee, H.-J., Inoue, K., Ida, H., Bouillet, P., Strasser, A., Bae, S.C., et al. (2006). The RUNX3 tumor suppressor upregulates Bim in gastric epithelial cells undergoing TGF-β-induced apoptosis. Mol. Cell. Biol. *26*, 4474–4488.